

# *Penetration impact testing of self-reinforced composites*

Meerten Y<sup>\*1</sup>, Swolfs Y<sup>1</sup>, Baets J<sup>1</sup>, Gorbatikh L<sup>1</sup>, Verpoest I<sup>1</sup>

<sup>1</sup> Department of Materials Engineering, KU Leuven, Kasteelpark Arenberg 44 bus 2450, Belgium

\*Corresponding author. Y. Meerten, Tel.: +32 16 37 35 12  
E-mail address: yannick.meerten@mtm.kuleuven.be (Meerten Y.)

## ***Abstract***

Penetration impact resistance is one of the key advantages of self-reinforced composites. This is typically measured using the same setup as for brittle fibre composites. However, issues with the test configuration for falling weight impact tests are reported. Similar issues have been found in literature for other composites incorporating ductile fibres. If the dimensions of the test samples are too small relative to the clamping device, then the test samples can heavily deform by wrinkling and necking. These unwanted mechanisms should be avoided as they absorb additional energy compared to properly tested samples. Furthermore, these mechanisms are found to occur more easily at lower compaction temperatures due to the lower interlayer bonding. In conclusions, the sample dimensions of ductile fibre composites should be carefully selected for penetration impact testing. If wrinkling or necking is observed, then the sample dimensions need to be increased.

## ***1. Introduction***

The number of applications for synthetic polymers continues to grow, because of their low density and generally low cost. They have replaced natural materials and metals in numerous applications. Their use is currently limited to non-structural applications due to their relatively low strength and stiffness. By adding a reinforcing fibre, these disadvantages can be mitigated. Glass, carbon and aramid fibres have been established as polymer reinforcements for several decades. However, these high performance fibres lead to composite failure strains ranging from 1 to 3%.

The mechanical properties of polymers can also be increased by inducing molecular orientation [1]. Polymers can for example be drawn into fibres or tapes [2-4]. These fibres and tapes can then be used to make self-reinforced composites (SRCs), where fibre and matrix are made of the same polymer. This type of composite with only one constituent was first investigated by Capiati and Porter [5]. Different production processes for self-reinforced composites were developed, such as hot compaction [6, 7], film stacking [8] and bicomponent tape technology [9, 10]. In the hot compaction technology, pressure and heat are applied to stacks of polymeric tapes. By selecting the optimal processing conditions, only the outer skin of the tapes melts, which forms the

matrix upon cooling. In the bicomponent tape technology, the polymeric tapes are coated with a copolymer, with a lower melting temperature. Upon compaction, only the copolymer is melted and subsequently forms the matrix cooling. Film stacking consists of adding polymer films in between layers of oriented polymer tapes or fibres. The films have a lower melting temperature than the oriented tape or fibre. The consolidation temperature is chosen between the melting temperature of the film and the oriented tape or fibre.

Extensive reviews of the production and mechanical properties of self-reinforced composites from different polymers can be found in [11, 12]. The mechanical properties of self-reinforced polypropylene (SRPP) depend on process parameters such as temperature, pressure and dwell time, and on material specific parameters such as weave architecture and tape draw ratio [13, 14]. The process temperature has a strong influence on the tensile properties of hot compacted SRPP: in a 12 °C temperature window, the strength increases from 55 MPa to 140 MPa and then falls back to 27 MPa [13]. Furthermore, higher temperatures increase the interlayer bonding [13, 15-17], which is typically quantified by the peel strength.

In addition to low density and recyclability, SRCs are attractive materials because of their excellent impact resistance. For characterization of the impact resistance, instrumented falling weight impact (IFWI) tests are common practice. IFWI tests are commonly used in literature to characterize the impact properties of SRPP [9, 18-23], but are actually only standardized for rigid plastics and brittle textile composites in ASTM 5628-96 [24] and ISO 6603-2 [25]. SRPP is more ductile and impact resistant than conventional glass or carbon fibre composites [6], and hence it is questionable whether SRPP can be properly tested using these standards.

Many authors published data for the penetration impact energy of SRPP. It is common practice to report values normalized by the thickness of the samples. However, Alcock et al. find a non-linear relation between the penetration impact energy and the thickness [9], so this normalization will induce an error on the following values. For hot compacted SRPP, penetration impact energies of 21 J/mm [20], 52-75 J/mm [19], and 26 J/mm [14] are reported. Bicomponent tape SRPP has an impact resistance of 20-44 J/mm [9], and finally for film stacked SRPP, values of 16-21 J/mm are reported [23].

Swolfs et al. [14] and Aurrekoetxea et al. [21] find that hot compacted SRPP primarily fails due to tape fracture, while delamination also significantly contributes to the energy absorption for the bicomponent tape SRPP [9]. For bicomponent tape SRPP, delaminations are more likely to occur according to Alcock et al. [9]. It is stated in [9] and [21] that increasing the consolidation temperature improves the interlayer bonding. A high interlayer bonding impedes the development of delaminations and therefore leads to more localized impact damage.

Alcock et al. [9], Crauwels [19] and Tissington et al. [26] show images of samples with severe deformation, such as those in Figure 1. The former two show images of SRPP

samples, while the latter shows that polyethylene fibre/epoxy composites can suffer from the same problem. Under normal circumstances, the main energy absorption mechanisms for SRPP during IFWI tests are tape fracture, delamination and debonding of fibre and matrix [9, 21, 23]. It is expected that heavily deformed samples will have a higher impact energy absorption, as the energy absorption mechanisms should be limited to inside the clamped region.

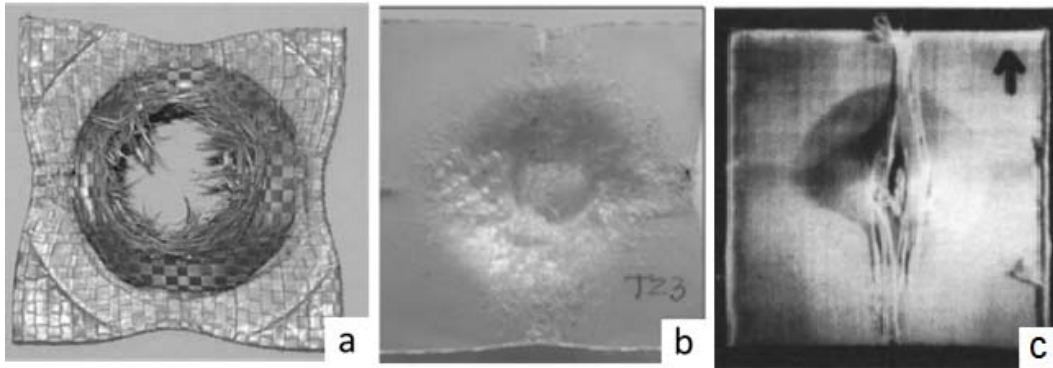


**Figure 1: Heavily deformed impact samples: (a) Alcock et al., bicomponent tape SRPP (reprinted from [9], with permission from Elsevier), (b) Crauwels, hot compacted SRPP [19], (c) Tissington et al., polyethylene-epoxy composite (reprinted from [26], with permission from Elsevier)**

The present work will investigate whether the standard IFWI test as performed in literature are applicable for ductile fibre composites. A number of assumptions made in literature need to be verified. Firstly, the compaction quality of the SRPP needs to be verified. Secondly, the linear relationship between penetration impact energy and sample thickness will be investigated, as Alcock et al. [9] indicate that this relationship is not linear. Thirdly, the influence of sample geometry and clamp size on the impact resistance is investigated and parameters for the evaluation of configuration-dependent behavior are proposed. Finally, when an adequate test setup is defined, the authors show the damage mechanisms change with the compaction temperature.

## **2. Materials and methods**

### **2.1. Materials**

Drawn polypropylene tapes are woven in a twill 2/2 pattern by Propex Fabrics GmbH (Germany). The tapes have a linear density of 110 tex, a stiffness of  $6.9 \pm 1.2$  GPa and a strength of  $589 \pm 24$  MPa [20]. Isotropic PP films of the same PP grade and with a thickness of 20  $\mu\text{m}$  were provided by Propex Fabrics GmbH.

### **2.2. Hot compaction**

To produce samples for impact testing, layers of woven PP-tapes with dimensions of 320x320 mm<sup>2</sup> were stacked between 1 mm thick aluminium plates. A Fontijne Grotnes LabPro400 hot press was pre-heated for 10 minutes at the compaction temperature to ensure a homogeneous temperature distribution. The stack was then inserted into the

press and kept at the compaction temperature and a pressure of 4 MPa for 5 minutes. During cooling to 40 °C in 5 minutes, the pressure was maintained to minimize shrinkage. To aid compaction, the woven PP tapes were interleaved with PP films for some layups. Unless otherwise mentioned, these films were not added.

Unless otherwise stated, the impact tests will be performed on 16 layers of SRPP compacted at 188 °C, without PP films. These samples have a thickness of 2.48 mm.

### ***2.3. Compaction quality***

Ultrasonic C-scans were performed to investigate the compaction quality, compacted at different temperatures. An Olympus Panametrics V309SU transducer at 5 MHz and 100 V and 13 mm nominal diameter was used for the scans. The step size was 2 mm and the plates were scanned at 0.2 mm/s. The histograms of the C-scans are processed with the signal processing algorithms by O'Haver [27] to differentiate between areas with a different compaction quality.

### ***2.4. Impact tests***

Instrumented falling weight impact (IFWI) tests are performed with different test setups, among which the ASTM D5628 and the ISO 6603-2 standards. A hemispherical striker with diameter 20 mm is used in combination with clamps with inner diameters of 40 and 80 mm and outer diameters of 60 and 100 mm, respectively. The samples are clamped with a force of 2800 N, regardless of the size of the clamp. This corresponds to a clamping pressure of 1780 kPa and 557 kPa for respectively the 60 mm and the 100 mm clamp. A striker with a weight of 26.17 kg is dropped from 1 m height, which is equivalent to an impact energy of 257 J. The penetration impact energy is calculated as the area underneath the force-displacement diagram until the force has dropped below half of its maximum value.

Unless otherwise stated, the square impact samples have a length of 100 mm and the default clamp is the one with an outer diameter of 60 mm. The compaction quality of every impact sample was verified with C-scanning. At least 5 impact samples were tested for each configuration.

## ***3. Results***

### ***3.1. Compaction quality assessment***

Scanning acoustic microscopy C-scans yield information about the homogeneity and compaction quality of the sample. The compaction quality is investigated on plates compacted at 184, 188 and 192 °C. These plates are square with a width of 320 mm and a thickness of  $2.48 \pm 0.03$  mm. The compaction quality will be evaluated by the histogram of reflected signal amplitude of the C-scan. A single, narrow peak at high greyscale value would indicate a homogeneous, high quality compaction.

Figure 2 and 3 respectively show the C-scan histograms and images of representative sample compacted at 184 °C, 188 °C and 192 °C. At 184 °C, the C-scan image shows that the compaction quality at the edges is considerably worse than in the middle of the plate. The horizontal and vertical lines found in the C-scan image correspond to the woven architecture. The dark grey areas correspond to the histogram at low greyscale values and indicate poor compaction quality. The middle of the plate on the other hand, shows a better compaction quality, corresponding to the peak at a greyscale of 117. The bimodality is caused by the inevitably lower temperature at the edges of the hot press, even though the press was stabilized at the compaction temperature for 10 minutes.

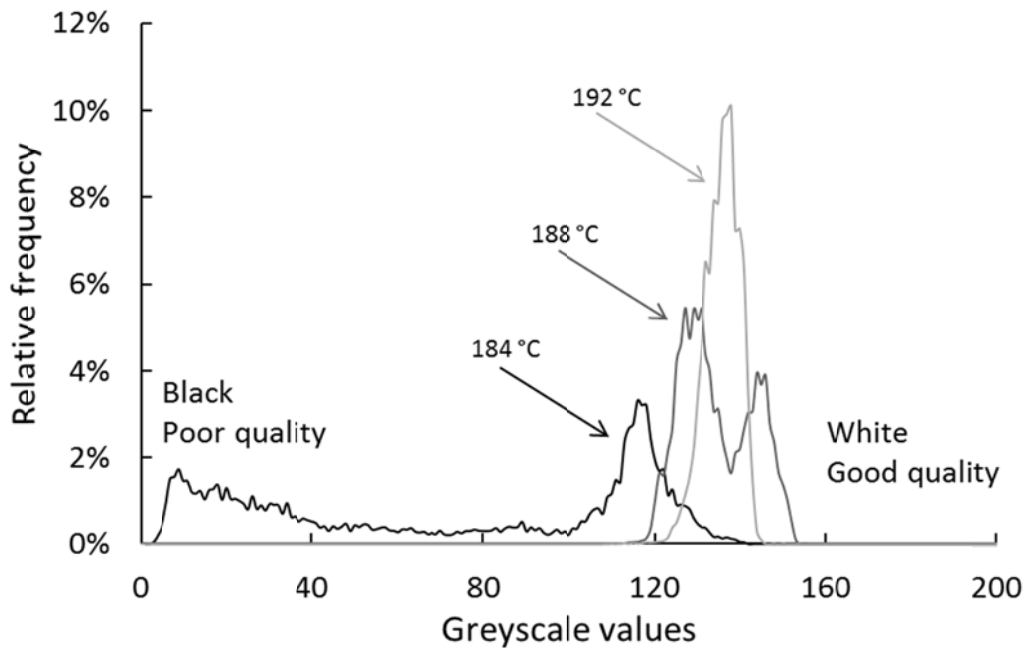


Figure 2: C-scan histograms of SRPP compacted three temperatures; greyscale 0 and 255 in the histogram represent respectively black and white in the image.

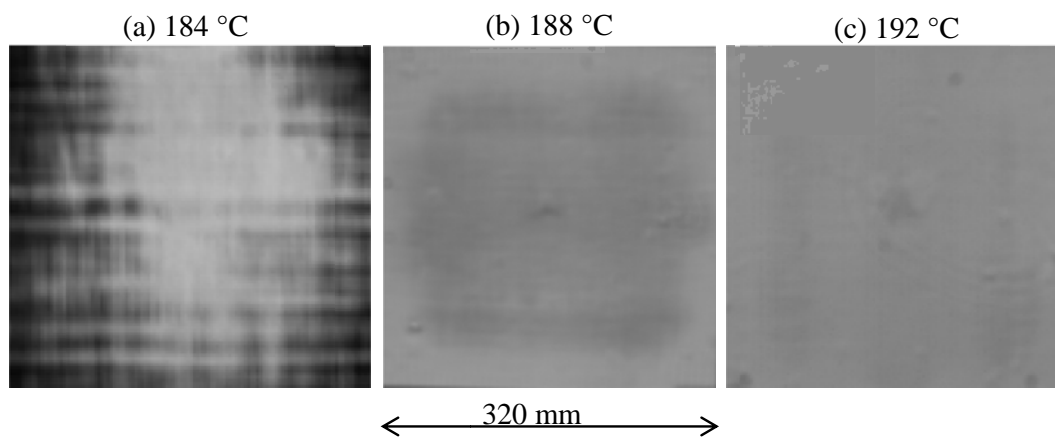


Figure 3: C-scan images of SRPP compacted at three temperatures: (a) 184 °C, (b) 188 °C, and (c) 192 °C. Black and white represent respectively bad and good compaction quality.

The compaction quality is significantly higher at 188 °C. The absence of a tail in Figure 2 implies that there are no large voids or dry areas in the material. Nevertheless, the histogram still shows a bimodal distribution, although both peaks have shifted to higher greyscales (better compaction quality). The C-scan image (see Figure 3b) indicates that the borders of the sample are whiter and thus better compacted than at 184 °C (see Figure 3a). This may have been caused by a higher shrinkage at the sample edges, causing more molecular relaxation and a local increase of the matrix fraction. This effect counteracts the lower temperature at the mould edge as observed for the 184 °C samples. The average greyscale is now 124 for the first peak and 142 for the second peak.

At 192 °C, a single, high peak is found, indicating homogeneous compaction quality. The bimodality has disappeared. A larger fraction of the tapes have melted at this temperature, as evidenced by the decrease in tensile strength and modulus [22].

From the investigation of the compaction quality, it is observed that the compaction quality at 184 °C is low and variable within one plate. At 188 °C, the compaction quality is higher, but still not completely homogeneous. Only at 192 °C, a completely homogeneous compaction is achieved. Impact samples will be cut from the samples in various locations. It is therefore expected that the scatter on the impact properties is inversely proportional to the compaction temperature.

### ***3.2. Effect of specimen thickness***

For a fair comparison between samples with different thicknesses, the absolute penetration impact energy is often normalized by the sample thickness. Normalization of the penetration impact energy assumes that the penetration impact energy of SRPP depends linearly on the sample thickness. Figure 4 validates this assumption, for SRPP compacted at 188 °C. A univariate regression shows a linear relation between penetration impact energy  $E_{pen}$  and thickness  $t$  with  $E_{pen}$  (J) = 26.8(J/mm) \*  $t$ (mm), with  $R^2 = 79.7\%$ .

It is also interesting to note that the penetration impact energy of a single layer follows this linear trend. Since a single layer cannot delaminate, most of the energy must be absorbed through tape fracture and perhaps some tape-matrix debonding. Tape fracture is hence the primary failure mechanism at 188 °C.

Figure 5 shows the decrease of thickness of a compacted plate with increasing compaction temperature for the same amount of layers. The difference between 184 °C and 188 °C is 4.6% and between 188 °C and 192 °C is 7.5%. Adding a PP film with a thickness of 20 µm between each layer of woven PP tapes gives a significant ( $p = 2.46\%$ ) increase in thickness of 5.0%. The film fills the remaining porosities in the composite, thus increasing the compaction quality. This is proven by the fact that the thickness only increases with 130 µm while the total added thickness of films is 300 µm.

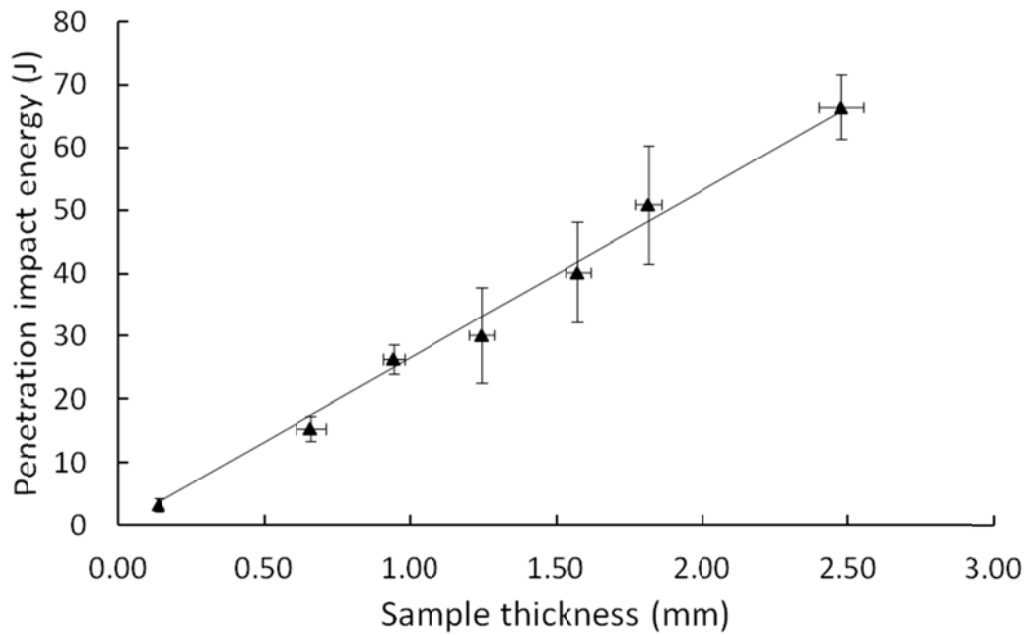


Figure 4: Linear relationship between penetration impact energy and the thickness of SRPP compacted at 188 °C.

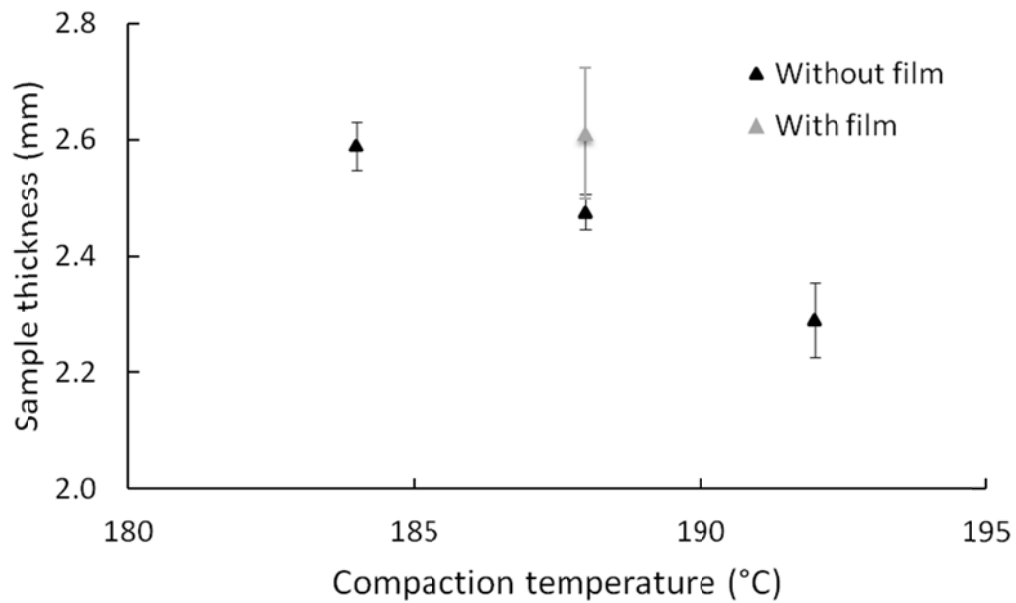


Figure 5: Thickness of 16 layers SRPP compacted at different temperatures.

In contrast with the linear trend in Figure 4, Alcock et al. [9] found a non-linear relationship between absolute impact resistance and sample thickness of bicomponent tape SRPP. The linear behavior was only observed for thickness values between 2.0 and 4.0 mm. At thicknesses below 2.0 mm, the impact resistance increased again. This trend

cannot continue as the impact resistance at 0 mm must be 0 J. Alcock et al. suggested that the non-linearity for bicomponent tape SRPP was caused by the increased deflection in thin samples. The images of the impacted samples (Figure 1a) shown by Alcock et al. in [9] show that some samples cannot resist deformation outside of the clamping area. It is likely more prevalent in lower thickness samples which are expected to have a lower geometrical stiffness. The next section changes the test geometry to investigate how deformation outside of the clamping area affects the penetration impact resistance.

### 3.3. Effect of test geometry

A robust testing technique in every scientific field should be independent of the test setup, or the influence of the testing environment should at least be understood. In literature, IFWI tests are performed on self-reinforced composites according to ASTM D5628 [24] and ISO 6603-2 [25]. These standards were developed for rigid plastics and brittle textile composites and are widely used for testing polymer composites. Conventional glass and carbon fibres are brittle, so their composites can be tested according to these standards. The same testing method should be used to allow a comparison between SRCs and conventional brittle fibre composites. However, it appears that two failure mechanisms are induced by the test setup, namely necking and wrinkling. Necking is defined as the in-plane deformation of the edges towards the center of the sample. Wrinkling is defined as out-of-plane deformation of sample. These damage mechanisms are observed when the samples have dimensions that are only slightly larger than the dimensions of the clamp. Examples of necking can be seen in Figure 1 and examples of wrinkling can be seen in Figure 6 and Figure 9.

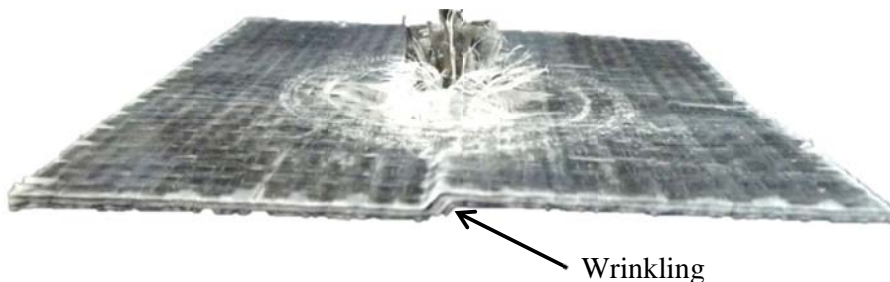


**Figure 6: Example of wrinkling observed in a slightly different SRPP composite.**

To verify whether the dimensions of the sample are sufficiently large compared to the clamp, the geometry ratio  $G$  is defined. This is computed as the edge length of the square sample divided by the outer diameter of the clamp. It is a measure for the excess amount of material that sticks outside of the clamp area. At a low geometry ratio  $G$ , necking and wrinkling will occur, leading to increased penetration energy. This deviation from a constant normalized penetration impact energy is shown in Figure 7.



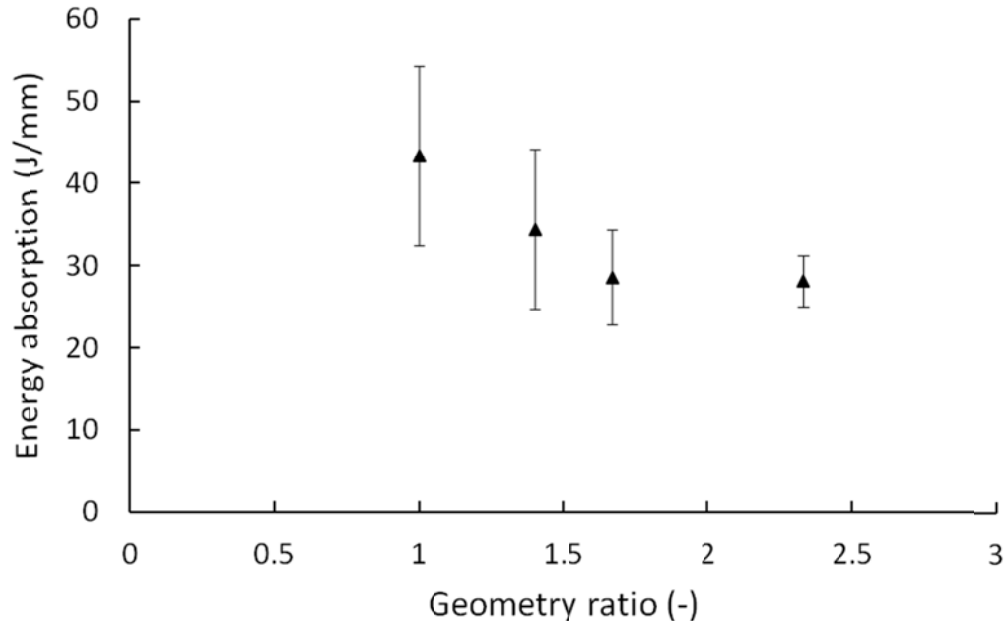


**Figure 7** Non-linear effect of the test geometry on the impact resistance of SRPP compacted at 188 °C.

The impact resistance at higher G ratios tends towards a stable value, where the excess amount of material is large enough to prevent any degree of necking and wrinkling. This is proven by an analysis on the variance (ANOVA) on the IFWI tests. Three sample lengths (60, 100, 140) are tested with the 60 mm clamp, giving G ratios of 1, 1.67 and 2.33. Similarly, four sample lengths (100, 140, 167, 233) are tested with the 100 mm clamp, giving G ratios of 1, 1.4, 1.67 and 2.33. Both the size of the clamp ( $P < 0.1\%$ ) and the size of the specimens ( $P < 1\%$ ) affect the penetration impact energy significantly.  $P < 0.1\%$  implies that the probability that the size of the clamp does not influence the penetration impact energy is smaller than 0.1%. The size of the clamp defines the volume of the material available for damage development. For the effect of the size of the specimens, the amount of material outside of the clamp needs to be considered, as this is the material that provides the resistance to necking and wrinkling. It is also found that an interaction between the two variables is unlikely ( $P = 10.7\%$ ).

Figure 7 also demonstrates the stabilization effect that larger geometry ratios have on the penetration impact energy. It is necessary to test samples that are significantly larger than the clamp. The additional material outside the clamps increases the resistance against unwanted deformation outside of the clamp, which is an artefact of the test geometry. At a certain geometry ratio, the resistance is sufficient to completely prevent these test geometry dependent deformation mechanisms. This is the minimal geometry ratio for adequate IFWI tests. For 16 layers of SRPP compacted at 188 °C, this ratio is around 1.67. These high geometry ratios also help to reduce the scatter in the measurements.

It should be noted that the 60 mm samples tested with the 60 mm clamp ( $G = 1$ ) can only be just clamped in, and of the 8 tested samples, only one is penetrated (Figure 8).

The other 7 are pulled into the clamp during the impact event. This is not the case for the 100 mm samples tested with the 100 mm clamp, where 5 out of 5 samples were penetrated. The authors believe that the larger clamping diameter allows more material to deform and absorb energy, because the deflection span is larger than for the 60 mm clamp.

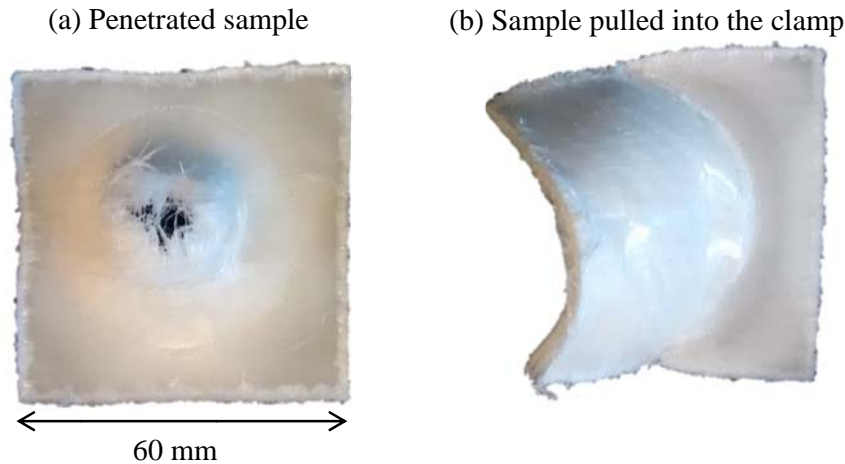


**Figure 8** Samples tested on the clamp with outer diameter 60 mm: (a) The only sample with penetration; (b) one of the eight samples that was pulled into the clamp.

Figure 9 shows samples compacted at 184 °C and geometry ratio 1.4 (140 mm sample / 100 mm clamp). 7 out of 8 samples did not penetrate due to heavy delaminations, caused by the weaker interface compared to samples compacted at 188°C. The delaminations grow under the clamp and lead to extensive wrinkling, as observed in all 8 tested samples. The in-plane deformation (necking) is limited because the sample is large enough to impede in-plane movement. This shows that samples compacted at 184 °C will have a higher minimal geometry ratio than samples compacted at 188 °C.

The effect of a weaker interface combined with a small geometry ratio is also visible in Figure 1a, where impacted samples of bicomponent tape SRPP show large necking. Note that the position of the clamp is clearly visible on the sample in Figure 1a, showing that the sample only just fitted in the clamp.

The authors believe that the effect of the test geometry is caused by imperfect fixation of the samples in the clamp. The penetration impact resistance of the composite would be independent of the amount of material outside the clamping ring if the clamping were perfect. A composite with low stiffness will have a tendency to wrinkle from the moment that any slip (imperfect fixation) is present. From that moment, it is beneficial to have surplus material outside of the clamps from the moment that any slip occurs.

In conclusion, care should be taken when testing ductile fibre composites. When necking or wrinkling is observed in such materials, the sample dimensions should be

increased. Alternatively, the size of the clamp can be increased, but then the size of the samples should be increased proportionally.

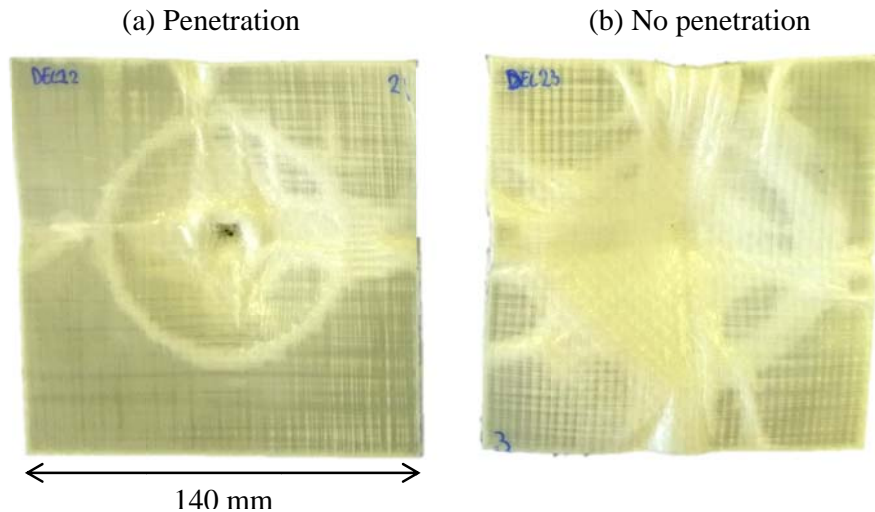
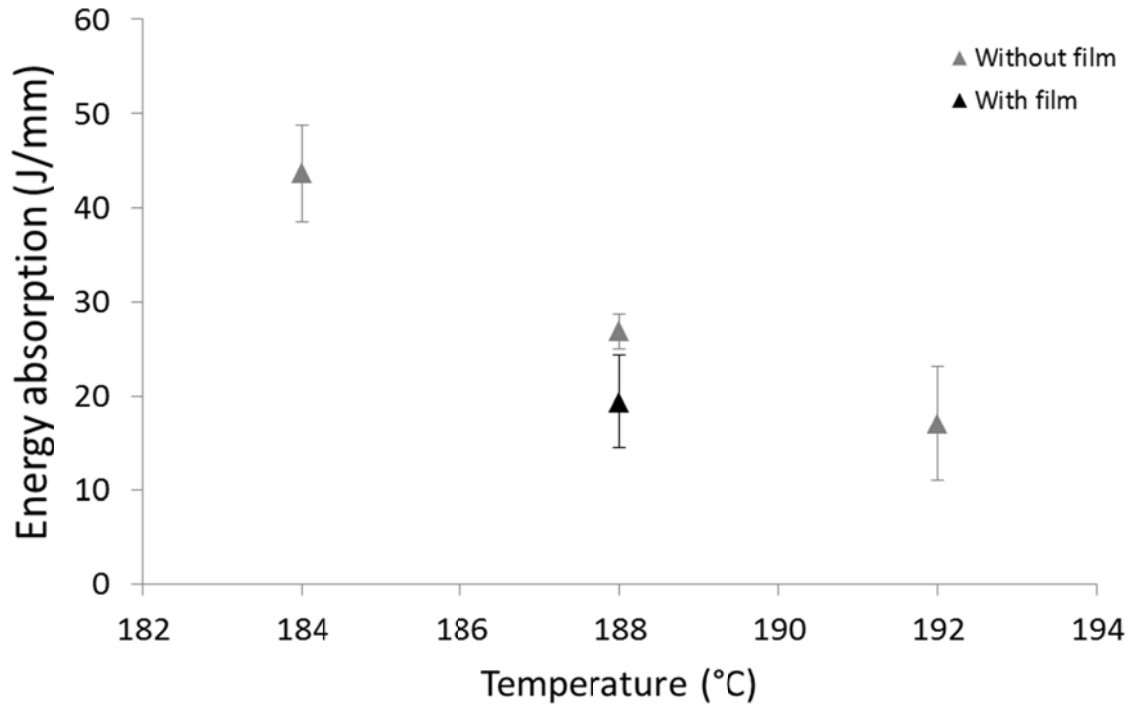


Figure 9 Impacted samples compacted at 184 °C, with the 100 mm clamp: a) the only sample out of 8 that was penetrated, and b) unpenetrated sample.

### 3.4. Effect of compaction temperature

Necking and wrinkling are more likely to occur with lower interlayer bonding. In hot compacted SRPP, the interlayer bonding strongly depends on the compaction temperature [13]. The influence of the processing temperature on the impact resistance of hot compacted SRPP is illustrated in Figure 10. The penetration impact energy drops from 44 J/mm to 17 J/mm by increasing the compaction temperature from 184°C to 192 °C. At higher temperatures, more relaxation of the PP-tapes is allowed and the amount of matrix material increases. This leads to increased interlayer bonding and composite failure strain but decreased tensile strength and tape failure strain [22]. The increase in interlayer bonding also impedes the development of delaminations. Hence, the penetration impact energy will decrease with increasing compaction temperature. For this investigation, samples with a size of 100 mm are tested with a clamp of 60 mm outer diameter ( $G = 1.67$ ).

The addition of films is a common practice to broaden the processing window of hot compaction [15]. The effect of the addition of films is similar to the effect of increasing the consolidation temperature. Adding one PP film between the woven PP layers, leads to a decrease of impact resistance of 36% at 188 °C. The improved adhesion hampers the development of delaminations. Furthermore, films increase the thickness of the composite plate by 5.2% while the additional matrix formed by the films only absorbs limited energy [20]. Hence, adding extra PP film between each woven PP layer lowers the normalized penetration impact energy.



**Figure 10** The influence of the compaction temperature and interleaved films on the impact performance.

Figure 11 displays representative penetrated samples at 184 °C, 188 °C (with and without extra PP films) and 192 °C. It is clear that the damage mechanisms leading to failure are different. The damage mechanisms considered are delamination, tape-matrix debonding and tape fracture. All these mechanisms show up as opaque areas in the images. It should be noted though, that plastic deformation of both tapes and matrix will lead to stress whitening in SRPP. The samples compacted at 188 °C still have a strong bonding between the layers after fracture. The samples compacted at 184 °C however, are heavily delaminated, as observed by bending the samples after impact. The area around the penetration that is severely damaged is smaller than for samples compacted at 184°C and limited to the area of the clamp. For samples compacted at 192 °C, a clean fracture in the two main directions of the underlying weave architecture is observed. Furthermore, the layers still adhere to each other after fracture. The use of interleaved film leads to an appearance intermediate to the samples compacted at 188 °C and 192 °C. Using interleaved films provides additional matrix material, increasing the resistance against delamination and debonding [15].

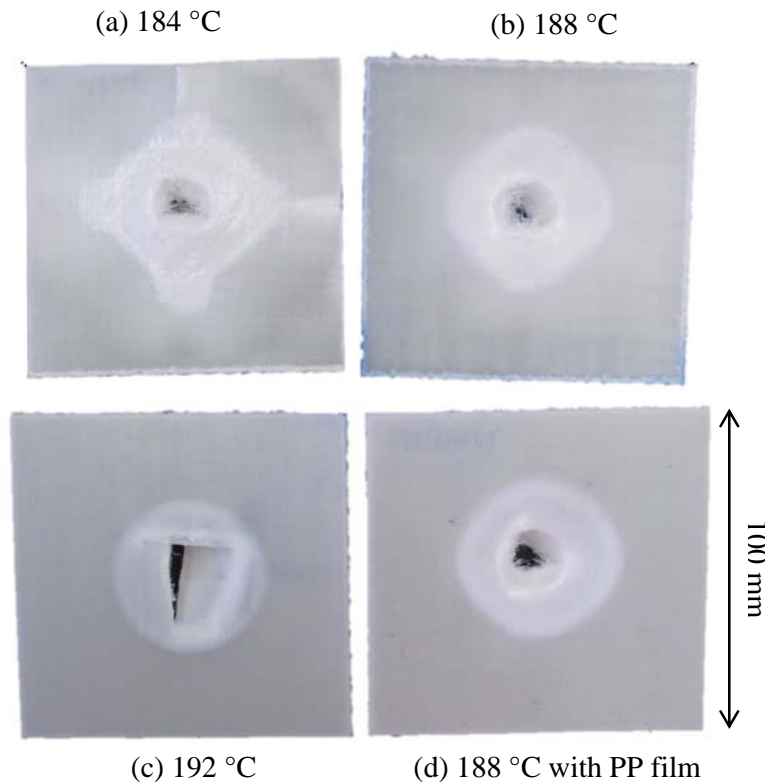


**Figure 11** Representative samples of penetrated SRPP a) compacted at 184 °C without interleaved film; b) compacted at 188 °C without interleaved film; c) compacted at 192 °C without interleaved film; d) compacted at 188 °C with interleaved film.

Tape-matrix debonding, delamination and tape fracture all contribute to the impact resistance. At 184 °C, visual inspection shows that delamination and tape-matrix debonding are the main failure mechanisms. It was found in section “3.2 Effect of specimen thickness” that at 188 °C, delamination is not contributing to the energy absorption anymore. At 192 °C, visual inspection shows that tape fracture is the dominant failure mechanism.

The sample compacted at 184 °C (see Figure 10a) shows wrinkling at the upper and right side. The investigation of the geometry ratio was performed with samples compacted at 188 °C in Chapter 3.3. This shows that the geometry ratio is temperature dependent. It is hypothesized that the difference in adhesion between 184 °C and 188 °C causes a change in damage development. Lower adhesion promotes delamination and tape-matrix debonding. It also allows the tapes directly under the striker to wrinkle. The relative contribution of these three damage mechanisms can unfortunately not be distinguished.

To conclude, this section describes that the damage mechanisms in SRPP depend on the compaction temperature. Because of the lower interlayer bonding, necking and wrinkling can occur more easily at lower compaction temperatures.

#### **4. Conclusion**

This paper finds a procedure for adequate testing of the penetration impact behavior of self-reinforced polypropylene. After verification of an adequate compaction quality at 188 °C, the assumption that the penetration impact energy can be normalized by the thickness, is validated. This is contrary to the behavior of bicomponent tape SRPP, where a non-linearity for the penetration impact energy as a function of the thickness is observed [9].

This non-linearity is caused by heavy deformation of the test samples. It is found that the impact resistance of SRPP is dependent on the sample size and clamp size in an IFWI test. It is necessary to have sufficient material outside the clamp to prevent unwanted failure mechanisms caused by inadequate test configurations. A geometry ratio  $G$  was defined as the ratio of the sample size divided by the clamp size. The penetration impact energy tends toward a stable value with increasing geometry ratio.

Some of the samples tested by Alcock et al. in [9], by Crauwels in [19] and by Tissington et al. in [26] have a geometry ratio close to 1, and the images in Figure 1 suggest the presence of similar, unwanted energy absorption mechanisms. Some of the values reported by Crauwels are overestimations of the impact resistance of hot compacted SRPP. It is likely that some of the values presented by Alcock et al. and Tissington et al. may also be overestimations, but this was not verified experimentally.

In general, when testing composites with ductile fibres, the geometry ratio should be sufficiently large to impede necking and wrinkling as damage mechanisms. The reported minimal geometry ratio of 1.67 for SRPP hot compacted at 188 °C cannot be generalized to other ductile fibres straight away. The minimal geometry ratio depends on various production parameters such as compaction temperature and material characteristics such as interlayer bonding and stiffness. Because so many parameters have an effect on the minimal geometry ratio, a general minimal geometry ratio for ductile fibre composites cannot be defined. Instead, when wrinkling or necking is observed in a ductile fibre composite, the size of the samples should be increased and the tests repeated. Alternatively, the size of the clamp can be increased, but then the size of the samples should be increased proportionally.

#### **5. Acknowledgments**

The authors thank the Agency for Innovation by Science and Technology in Flanders (IWT) for the grant of Y. Swolfs. I. Verpoest holds the Toray Chair in Composite Materials at KU Leuven.

## 6. References

- [1] Alcock B, Cabrera NO, Barkoula NM, Peijs T. The effect of processing conditions on the mechanical properties and thermal stability of highly oriented PP tapes. *European Polymer Journal*. 2009;45(10):2878-94.
- [2] McHugh AJ, Guy RK, Tree DA. Extensional flow-induced crystallization of a polyethylene melt. *Colloid Polym Sci*. 1993;271(7):629-45.
- [3] Lee IH, Schultz JM. Adhesion in laminates of highly oriented polypropylene sheets. *Polymer*. 1986;27(8):1219-27.
- [4] Bigg DM. Mechanical property enhancement of semicrystalline polymers - a review. *Polym Eng Sci*. 1988;28(13):830-55.
- [5] Capiati NJ, Porter RS. Concept of one polymer composites modeled with high-density polyethylene. *Journal of Materials Science*. 1975;10(10):1671-7.
- [6] Ward IM, Hine PJ. The science and technology of hot compaction. *Polymer*. 2004;45(5):1413-27.
- [7] Hine PJ, Ward IM, Olley RH, Bassett DC. The hot compaction of high modulus melt-spun polyethylene fibers. *Journal of Materials Science*. 1993;28(2):316-24.
- [8] Zhang JM, Reynolds CT, Peijs T. All-poly(ethylene terephthalate) composites by film stacking of oriented tapes. *Compos Pt A-Appl Sci Manuf*. 2009;40(11):1747-55.
- [9] Alcock B, Cabrera NO, Barkoula NM, Peijs T. Low velocity impact performance of recyclable all-polypropylene composites. *Composites Science and Technology*. 2006;66(11-12):1724-37.
- [10] Cabrera N, Alcock B, Loos J, Peijs T. Processing of all-polypropylene composites for ultimate recyclability. *Proc Inst Mech Eng Pt L-J Mater-Design Appl*. 2004;218(L2):145-55.
- [11] Alcock B, Peijs T. Technology and Development of Self-Reinforced Polymer Composites. In: Abe A, Kausch H-H, Möller M, Pasch H, editors. *Polymer Composites – Polyolefin Fractionation – Polymeric Peptidomimetics – Collagens*: Springer Berlin Heidelberg; 2013. p. 1-76.
- [12] Karger-Kocsis J, Barany T. *Single-Polymer Composites (SPCs): Status and Future Trends*. Composites Science and Technology. 2013.
- [13] Hine PJ, Ward IM, Jordan ND, Olley R, Bassett DC. The hot compaction behaviour of woven oriented polypropylene fibres and tapes. I. Mechanical properties. *Polymer*. 2003;44(4):1117-31.
- [14] Swolfs Y, Crauwels L, Gorbatikh L, Verpoest I. The influence of weave architecture on the mechanical properties of self-reinforced polypropylene. *Compos Pt A-Appl Sci Manuf*. 2013;53:129-36.

- [15] Hine PJ, Ey RH, Ward IM. The use of interleaved films for optimising the production and properties of hot compacted, self reinforced polymer composites. *Composites Science and Technology*. 2008;68(6):1413-21.
- [16] Alcock B, Cabrera NO, Barkoula NM, Spoelstra AB, Loos J, Peijs T. The mechanical properties of woven tape all-polypropylene composites. *Compos Pt A-Appl Sci Manuf*. 2007;38(1):147-61.
- [17] Hine PJ, Unwin AP, Ward IM. The use of an interleaved film for optimising the properties of hot compacted polyethylene single polymer composites. *Polymer*. 2011;52(13):2891-8.
- [18] Alcock B, Cabrera NO, Barkoula NM, Wang Z, Peijs T. The effect of temperature and strain rate on the impact performance of recyclable all-polypropylene composites. *Compos Pt B-Eng*. 2008;39(3):537-47.
- [19] Crauwels L. Intralayer hybridization of self-reinforced composites, Master Thesis: KULeuven; 2012.
- [20] Swolfs Y, Van den fonteyne W, Baets J, Verpoest I. Failure behaviour of self-reinforced polypropylene at and below room temperature. *Composites Part A: Applied Science and Manufacturing*. 2014;65(0):100-7.
- [21] Aurrekoetxea J, Sarrionandia M, Mateos M, Aretxabaleta L. Repeated low energy impact behaviour of self-reinforced polypropylene composites. *Polymer Testing*. 2011;30(2):216-21.
- [22] Swolfs Y, Zhang Q, Baets J, Verpoest I. The influence of process parameters on the properties of hot compacted self-reinforced polypropylene composites. *Composites Part A: Applied Science and Manufacturing*. 2014;65(0):38-46.
- [23] Bárány T, Izer A, Karger-Kocsis J. Impact resistance of all-polypropylene composites composed of alpha and beta modifications. *Polymer Testing*. 2009;28(2):176182.
- [24] ASTM D5628-96: Standard Test Method for Impact Resistance of Flat, Rigid Plastic Specimens by Means of a Falling Dart. 2001.
- [25] ISO 6630-2 Plastics - Determination of puncture impact behaviour of rigid plastics - Part 2: Instrumented impact testing. 2000.
- [26] Tissington B, Pollard G, Ward IM. A study on the impact behavior of ultra-high-modulus polyethylene fiber composites. *Composites Science and Technology*. 1992;44(3):197-208.
- [27] O'Haver T. *A Pragmatic Introduction to Signal Processing*. 2014.